

000 001 002 003 004 005 006 007 008 009 010 011 012 013 014 015 016 017 018 019 020 021 022 023 024 025 026 027 028 029 030 031 032 033 034 035 036 037 038 039 040 041 042 043 044 045 046 047 048 049 050 051 052 053 ENHANCING LINEAR ATTENTION WITH RESIDUAL LEARNING

Anonymous authors

Paper under double-blind review

ABSTRACT

Linear attention offers a linear-time alternative to self-attention but often struggles to capture long-range patterns. We revisit linear attention through a prediction-correction lens and show that prevalent variants can be written as a combination of a historical prediction and a single-token correction, which creates an expressivity bottleneck. To address this bottleneck, we introduce **Residual Linear Attention (RLA)**, a framework that equips linear attention with an explicit *residual-fitting* mechanism. RLA maintains an auxiliary recurrent state that learns to accumulate residual errors over time and correct the base prediction. We further instantiate a delta-rule version, **Residual Delta Net (RDN)**, incorporating adaptive gating and residual clipping for enhanced correction control and stability. Our implementation leverages highly optimized linear attention kernels and preserves linear time and memory. Across language modeling and recall-intensive evaluations, RLA and RDN consistently outperform their respective baselines and other modern linear-attention methods, narrowing the gap to standard Transformers while retaining linear scaling.

1 INTRODUCTION

The Transformer (Vaswani et al., 2017) architecture has become the standard for large language models. However, the quadratic time complexity of its self-attention mechanism remains a critical bottleneck, limiting its application to long sequences (Li et al., 2024). Linear attention has recently emerged as an efficient alternative to standard self-attention, directly addressing its prohibitive quadratic complexity. By reformulating the attention computation into a recurrent process, these models achieve linear-time training and inference, making them well-suited for processing long sequences. Architectures such as RetNet (Sun et al., 2023) and Mamba (Gu & Dao, 2023; Dao & Gu, 2024) have demonstrated competitive performances. Methods like GLA (Yang et al., 2023) and DeltaNet (Yang et al., 2024b) offer further improvements by incorporating data-dependent gating and state update rules to manage the flow of information within a single state matrix.

Modern linear attention methods can be unified as learning a direct mapping from keys to values (Sun et al., 2024), a process analogous to test-time training. For example, the delta update rule (Schlag et al., 2021) can be derived from a single step of online gradient descent on a quadratic loss objective. This perspective opens several avenues for improvement. These include exploring different online learning loss functions to derive new update rules (Schlag et al., 2021; Yang et al., 2024b), employing more sophisticated mapping functions, or modifying the online gradient update mechanism (von Oswald et al., 2025; Siems et al., 2025). For instance, recent works like TTT-MLP (Sun et al., 2024) and Titans (Behrouz et al., 2024) utilize a Multi-Layer Perceptron (MLP) as a deep memory module to achieve a more powerful mapping. However, this approach sacrifices the model’s linear recurrence, thereby complicating parallel training.

Building on this perspective, we offer a new interpretation of the attention output. We show that the output of prevalent linear attention models can be decomposed into a base component generated from historical states and a correction term derived solely from the current token (see Section 2.3). Relying on a single token to perform this systematic correction imposes a bottleneck and is detrimental to the model’s expressive power. To address these issues, we introduce Residual Linear Attention, a framework that enhances linear attention models with an explicit residual fitting mechanism. Rather than depending on a single token for correction, our method employs an auxiliary state

matrix to explicitly model and correct systematic prediction errors of the base linear attention. The final output is a combination of the base prediction and this learned error correction. Our approach can be generalized to a unified framework applicable to various linear attention methods, offering a powerful and efficient strategy for building more capable sequence models.

Building upon existing linear attention methods, we propose two variants enhanced with residual fitting: Residual Linear Attention (RLA) and Residual Delta Net (RDN). We evaluate them on a range of benchmarks, including language modeling and recall-intensive tasks. Our results demonstrate that these models outperform their respective baselines and other modern linear attention methods, while our ablation analysis confirms the importance of each key design choice within our framework.

2 PRELIMINARIES

2.1 LINEAR ATTENTION AS A RECURRENT MODEL

Softmax attention mechanisms exhibit quadratic computational complexity with respect to sequence length, constituting a significant bottleneck when processing long sequences. Linear attention (Katharopoulos et al., 2020) architectures address this by removing the softmax function, which allows for a reordering of the computation.

For the t -th token in a sequence, let the query, key, and value vectors be $\mathbf{q}_t \in \mathbb{R}^{d_q \times 1}$, $\mathbf{k}_t \in \mathbb{R}^{d_k \times 1}$, and $\mathbf{v}_t \in \mathbb{R}^{d_v \times 1}$, where d_q , d_k , and d_v are their respective feature dimensions, with $d_q = d_k$. After applying a kernel function $\phi(\cdot)$ to the queries and keys (omitted for simplicity in the notation), the causal linear attention output \mathbf{o}_t can be expressed as:

$$\mathbf{o}_t = \sum_{i=1}^t \mathbf{v}_i (\mathbf{k}_i^\top \mathbf{q}_t) = \left(\sum_{i=1}^t \mathbf{v}_i \mathbf{k}_i^\top \right) \mathbf{q}_t.$$

By defining a state matrix $\mathbf{S}_t := \sum_{i=1}^t \mathbf{v}_i \mathbf{k}_i^\top \in \mathbb{R}^{d_v \times d_k}$, we arrive at the following recurrent formulation:

$$\mathbf{S}_t = \mathbf{S}_{t-1} + \mathbf{v}_t \mathbf{k}_t^\top, \quad \mathbf{o}_t = \mathbf{S}_t \mathbf{q}_t.$$

This recurrent form maintains constant time and memory complexity per step during inference and facilitates efficient training through chunk-wise parallel algorithms (Yang et al., 2023). Furthermore, the use of gating mechanisms has led to the development of more variants such as RetNet (Sun et al., 2023), Lightning Attention (Qin et al., 2024a), and Mamba-2 (Dao & Gu, 2024).

2.2 AN ONLINE LEARNING PERSPECTIVE

The design of the recurrent update rule can be motivated from an online learning perspective (Sun et al., 2024; Liu et al., 2024). In this view, the token sequence is a stream of data points $(\mathbf{k}_t, \mathbf{v}_t)$, and the state matrix \mathbf{S} acts as model parameters. These parameters are updated online to learn the mapping $\mathbf{k} \mapsto \mathbf{v}$, with \mathbf{S} functioning as a memory from which information is retrieved using the query \mathbf{q} via $\mathbf{S}\mathbf{q}$.

The state update can be interpreted as one step of gradient descent on a loss function $\mathcal{L}(\mathbf{k}, \mathbf{v}; \mathbf{S})$. For instance, applying a single descent step with the loss $\mathcal{L}(\mathbf{k}_t, \mathbf{v}_t; \mathbf{S}) := -\langle \mathbf{S}\mathbf{k}_t, \mathbf{v}_t \rangle$ recovers the standard linear attention update:

$$\mathbf{S}_t = \mathbf{S}_{t-1} - \nabla_{\mathbf{S}} \mathcal{L}(\mathbf{k}_t, \mathbf{v}_t; \mathbf{S}_{t-1}) = \mathbf{S}_{t-1} + \mathbf{v}_t \mathbf{k}_t^\top.$$

An alternative update rule can be derived by minimizing a squared error loss, $\mathcal{L}(\mathbf{k}_t, \mathbf{v}_t; \mathbf{S}) := \frac{1}{2} \|\mathbf{S}\mathbf{k}_t - \mathbf{v}_t\|^2$. Performing one step of gradient descent on \mathbf{S}_{t-1} with a data-dependent learning rate β_t yields the delta rule:

$$\mathbf{S}_t = \mathbf{S}_{t-1} - \beta_t \nabla_{\mathbf{S}} \mathcal{L}(\mathbf{k}_t, \mathbf{v}_t; \mathbf{S}_{t-1}) = \mathbf{S}_{t-1} (I - \beta_t \mathbf{k}_t \mathbf{k}_t^\top) + \beta_t \mathbf{v}_t \mathbf{k}_t^\top.$$

This formulation enables models like Delta Net (Yang et al., 2024b; Schlag et al., 2021) to achieve fine-grained memory control. Gated Delta Net (Yang et al., 2024a) further enhances this approach by incorporating weight decay into the learning process.

108 2.3 DECOMPOSITION INTO PREDICTION AND CORRECTION
109110 We interpret linear attention through a prediction-correction lens. The standard linear attention
111 output, $\mathbf{o}_t = \mathbf{S}_t \mathbf{q}_t$, can be viewed as the sum of a base prediction from the past state and a correction
112 based on the current token:

113
$$\mathbf{o}_t = \underbrace{\mathbf{S}_{t-1} \mathbf{q}_t}_{\text{Base Prediction}} + \underbrace{(\mathbf{v}_t \mathbf{k}_t^\top) \mathbf{q}_t}_{\text{Error Correction}}.$$

114
115

116 We can generalize this decomposition to the form $\mathbf{o}_t = \mathbf{S}_{t-1} \mathbf{q}_t + \mathbf{R}_t \mathbf{q}_t$, where we introduce \mathbf{R}_t
117 as a generalized correction state. This framework provides a unified view of several methods, as
118 shown in Table 1, which differ not only in the design of their associated state update but also in this
119 correction term.120 Table 1: Comparison of different linear attention methods with base prediction and error correction.
121

Method	Output Combination	State Update Rule	Correction Term
LinearAttn	$\mathbf{o}_t = \mathbf{S}_{t-1} \mathbf{q}_t + \mathbf{R}_t \mathbf{q}_t$	$\mathbf{S}_t = \mathbf{S}_{t-1} + \mathbf{v}_t \mathbf{k}_t^\top$	$\mathbf{R}_t = \mathbf{v}_t \mathbf{k}_t^\top$
Mamba2	$\mathbf{o}_t = \alpha_t \mathbf{S}_{t-1} \mathbf{q}_t + \mathbf{R}_t \mathbf{q}_t$	$\mathbf{S}_t = \alpha_t \mathbf{S}_{t-1} + \mathbf{v}_t \mathbf{k}_t^\top$	$\mathbf{R}_t = \mathbf{v}_t \mathbf{k}_t^\top$
Gated LinearAttn	$\mathbf{o}_t = \text{diag}(\alpha_t) \mathbf{S}_{t-1} \mathbf{q}_t + \mathbf{R}_t \mathbf{q}_t$	$\mathbf{S}_t = \text{diag}(\alpha_t) \mathbf{S}_{t-1} + \mathbf{v}_t \mathbf{k}_t^\top$	$\mathbf{R}_t = \mathbf{v}_t \mathbf{k}_t^\top$
DeltaNet	$\mathbf{o}_t = \mathbf{S}_{t-1} \mathbf{q}_t + \beta_t \mathbf{R}_t \mathbf{q}_t$	$\mathbf{S}_t = \mathbf{S}_{t-1} (I - \beta_t \mathbf{k}_t \mathbf{k}_t^\top) + \beta_t \mathbf{v}_t \mathbf{k}_t^\top$	$\mathbf{R}_t = (\mathbf{v}_t - \mathbf{S}_{t-1} \mathbf{k}_t) \mathbf{k}_t^\top$
Gated DeltaNet	$\mathbf{o}_t = \alpha_t \mathbf{S}_{t-1} \mathbf{q}_t + \beta_t \mathbf{R}_t \mathbf{q}_t$	$\mathbf{S}_t = \alpha_t \mathbf{S}_{t-1} (I - \beta_t \mathbf{k}_t \mathbf{k}_t^\top) + \beta_t \mathbf{v}_t \mathbf{k}_t^\top$	$\mathbf{R}_t = (\mathbf{v}_t - \alpha_t \mathbf{S}_{t-1} \mathbf{k}_t) \mathbf{k}_t^\top$

132 Building on the prediction-correction viewpoint, we introduce a residual fitting framework to en-
133 hance linear attention. Our framework learns a more expressive correction term by explicitly fitting
134 on contextual information beyond the current token.

136 3 METHOD

139 This section presents our proposed method, which enhances linear attention through a residual-
140 fitting process. We begin by describing the foundational residual learning framework that underpins
141 our method. Next, we introduce an adaptive correction factor to enhance modeling capabilities and
142 clipping methods to stabilize the residual fitting process. Finally, we present two final variants of
143 our approach.

144 3.1 EXPLICIT RESIDUAL FITTING

146 As established in Section 2.3, the output of linear attention can be decomposed into a base prediction
147 and a correction term. To learn a more expressive correction, we introduce an auxiliary state, \mathbf{R}_t ,
148 which modifies the output formulation to $\mathbf{o}_t = \mathbf{S}_{t-1} \mathbf{q}_t + \mathbf{R}_t \mathbf{q}_t$. Crucially, unlike the standard
149 correction shown in Table 1, which is derived solely from the current token, our auxiliary state \mathbf{R}_t
150 is updated recurrently, analogous to the primary state \mathbf{S}_t .151 The learning target for state \mathbf{R}_t is motivated by a second-order analysis of the loss function. Given
152 a prediction $\hat{\mathbf{v}}$, the Taylor expansion of a loss function $\mathcal{L}(\hat{\mathbf{v}}, \mathbf{v})$ around $\hat{\mathbf{v}}$ with a small perturbation δ
153 is:

154
$$\mathcal{L}(\hat{\mathbf{v}} + \delta, \mathbf{v}) \approx \mathcal{L}(\hat{\mathbf{v}}, \mathbf{v}) + (\nabla_{\hat{\mathbf{v}}} \mathcal{L})^\top \delta + \frac{1}{2} \delta^\top (\nabla_{\hat{\mathbf{v}}}^2 \mathcal{L}) \delta.$$

155

156 Minimizing this approximation with respect to δ suggests an optimal update step, $\delta^* = -(\nabla_{\hat{\mathbf{v}}}^2 \mathcal{L})^{-1} (\nabla_{\hat{\mathbf{v}}} \mathcal{L})$. For the commonly used L2 loss, $\mathcal{L} = \frac{1}{2} \|\mathbf{v} - \hat{\mathbf{v}}\|^2$, this optimal update sim-
157 plifies directly to the residual error, $\mathbf{r} := \delta^* = \mathbf{v} - \hat{\mathbf{v}}$. This motivates modeling the residual with our
158 auxiliary state, which we define as $\mathbf{r}_t := \mathbf{v}_t - \mathbf{S}_{t-1} \mathbf{k}_t$.159 161 Leveraging the online learning perspective of linear attention from Section 2, we apply an analogous
160 update rule to the auxiliary state. This yields the following recurrent process:

162
163 $\mathbf{r}_t = \mathbf{v}_t - \mathbf{S}_{t-1} \mathbf{k}_t$ (Residual Error Computation)
164
165 $\mathbf{R}_t = \mathbf{R}_{t-1} + \mathbf{r}_t \mathbf{k}_t^\top$ (Auxiliary State Update)
166
167 $\mathbf{o}_t = \mathbf{S}_{t-1} \mathbf{q}_t + \mathbf{R}_t \mathbf{q}_t$ (Output Combination)
168
169 $\mathbf{S}_t = \mathbf{S}_{t-1} + \mathbf{v}_t \mathbf{k}_t^\top$ (Base State Update)

170 In this formulation, the auxiliary state \mathbf{r}_t accumulates past residual errors and their corresponding
171 keys. This allows it to model and correct for systematic prediction errors made by the base state
172 \mathbf{S}_{t-1} , yielding a more expressive output. Furthermore, we generalize this residual fitting process
173 to formulate a unified framework for boosting linear attention, with a detailed derivation provided
174 in Appendix A.

175 It is worth noting two special cases of this formulation. If we set $\mathbf{R}_t = \mathbf{v}_t \mathbf{k}_t^\top$, using information
176 only from the current token, our method reduces to standard linear attention (Katharopoulos et al.,
177 2020). If we instead use $\mathbf{R}_t = (\mathbf{v}_t - \mathbf{S}_{t-1} \mathbf{k}_t) \mathbf{k}_t^\top$, the correction mechanism becomes equivalent to
178 a one-step delta rule update (Schlag et al., 2021).

180 3.2 ADAPTIVE GATING AND CORRECTION FACTOR
181

182 To enhance control over the state dynamics, we incorporate learnable gating scalars, a practice
183 common in recent recurrent models (Yang et al., 2024a; Dao & Gu, 2024). We introduce a decay
184 factor $\alpha_t \in [0, 1]$ to control the retention of past information, and an update rate $\beta_t \in [0, 1]$ to
185 modulate the influence of the current token. These factors can be applied to both state updates and
186 output combinations:

187 $\mathbf{S}_t = \alpha_t \mathbf{S}_{t-1} + \beta_t \mathbf{v}_t \mathbf{k}_t^\top$
188
189 $\mathbf{R}_t = \alpha_t \mathbf{R}_{t-1} + \beta_t \mathbf{r}_t \mathbf{k}_t^\top$
190
191 $\mathbf{o}_t = \alpha_t \mathbf{S}_{t-1} \mathbf{q}_t + \beta_t \mathbf{R}_t \mathbf{q}_t$

192 However, using the same update rate β_t for both states couples the learning of the base representation
193 and the error correction. To achieve more fine-grained control, we introduce a dedicated scalar
194 correction factor, $\gamma_t \in [0, 1]$. This factor decouples the update processes and allows the model to
195 dynamically scale the contribution of the residual correction term. The auxiliary state updates and
196 output computation are given by:

197 $\mathbf{S}_t = \alpha_t \mathbf{S}_{t-1} + \beta_t \mathbf{v}_t \mathbf{k}_t^\top$
198
199 $\mathbf{R}_t = \alpha_t \mathbf{R}_{t-1} + \gamma_t \mathbf{r}_t \mathbf{k}_t^\top$
200
201 $\mathbf{o}_t = \alpha_t \mathbf{S}_{t-1} \mathbf{q}_t + \gamma_t \mathbf{R}_t \mathbf{q}_t$

203 This formulation uses the decay and correction factors to dynamically gate the retrieval from the
204 base and auxiliary states, respectively.

206 3.3 NORMALIZATION AND RESIDUAL CLIPPING
207

208 To ensure computational stability, we introduce two mechanisms. First, we apply L2 normalization
209 to the query and key vectors to improve numerical stability. Second, we address potential instability
210 in the auxiliary state \mathbf{r}_t by clipping the residual:

211 $\mathbf{r}_t = \text{Clip}_{[-c, c]}(\mathbf{v}_t - \mathbf{S}_{t-1} \mathbf{k}_t).$

214 This ensures that the error-correction state \mathbf{r}_t maintains a stable learning trajectory, even when the
215 base model produces transient, large prediction errors. A detailed derivation for this clipping method
is provided in Appendix B.

216 3.4 FINAL FORMULATIONS
217

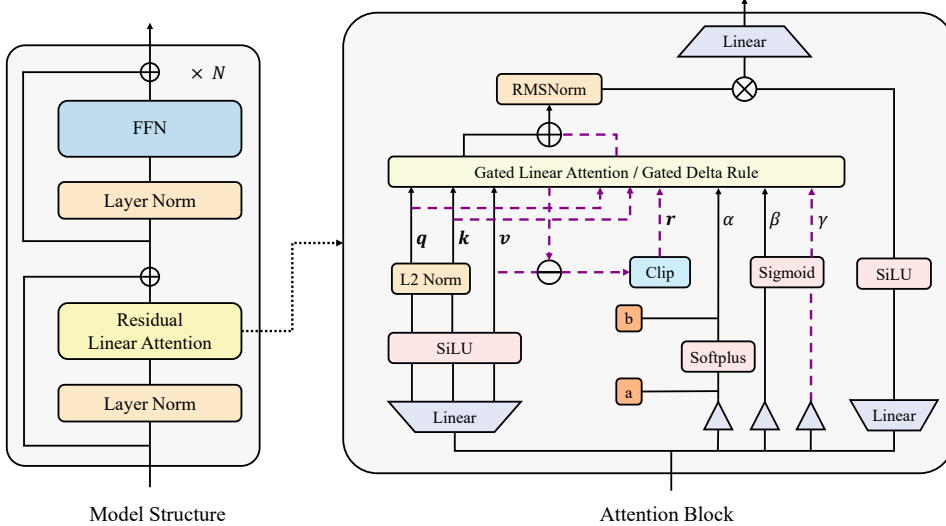
218 The residual fitting principle is a general technique that can be integrated with various linear attention
219 backbones. By applying our residual mechanism to both the standard additive update rule and the
220 delta update rule, we derive two powerful variants. This leads to our final models:
221
222

$$\begin{aligned} 223 \quad \mathbf{r}_t &= \text{Clip}_{[-c, c]}(\mathbf{v}_t - \mathbf{S}_{t-1} \mathbf{k}_t) \\ 224 \quad \mathbf{R}_t &= \alpha_t \mathbf{R}_{t-1} + \gamma_t \mathbf{r}_t \mathbf{k}_t^\top \\ 225 \quad \mathbf{S}_t &= \alpha_t \mathbf{S}_{t-1} + \beta_t \mathbf{v}_t \mathbf{k}_t^\top \\ 226 \quad \mathbf{o}_t &= \alpha_t \mathbf{S}_{t-1} \mathbf{q}_t + \gamma_t \mathbf{R}_t \mathbf{q}_t \end{aligned}$$

$$\begin{aligned} 223 \quad \mathbf{r}_t &= \text{Clip}_{[-c, c]}(\mathbf{v}_t - \mathbf{S}_{t-1} \mathbf{k}_t) \\ 224 \quad \mathbf{R}_t &= \alpha_t \mathbf{R}_{t-1} (I - \gamma_t \mathbf{k}_t \mathbf{k}_t^\top) + \gamma_t \mathbf{r}_t \mathbf{k}_t^\top \\ 225 \quad \mathbf{S}_t &= \alpha_t \mathbf{S}_{t-1} (I - \beta_t \mathbf{k}_t \mathbf{k}_t^\top) + \beta_t \mathbf{v}_t \mathbf{k}_t^\top \\ 226 \quad \mathbf{o}_t &= \alpha_t \mathbf{S}_{t-1} \mathbf{q}_t + \gamma_t \mathbf{R}_t \mathbf{q}_t \end{aligned}$$

227 **Residual Linear Attention (RLA)**228 **Residual Delta Net (RDN)**

229 For brevity, the equations omit the L2 normalization and SiLU activation applied to query and key
230 vectors. Regarding the adaptive gates, the decay factor α_t adopts the re-parameterization from
231 Mamba-2 (Dao & Gu, 2024), while β_t and γ_t are computed via a linear projection followed by a
232 sigmoid activation. The structure of our attention block is shown in Figure 1.



233 Figure 1: The architecture of our proposed model. The model structure (left) consists of N stacked blocks. The
234 detailed Attention Block (right) illustrates our core mechanism. Our primary contribution, the explicit residual
235 fitting process, is highlighted in purple dash lines. This path computes the clipped residual $\mathbf{r}_t = \text{Clip}(\mathbf{v}_t -$
236 $\mathbf{S}_{t-1} \mathbf{k}_t)$, which is then modulated by a dedicated correction factor $\gamma_t = \sigma(\mathbf{W}_\gamma \mathbf{x})$ to dynamically correct the
237 base prediction from the model’s primary state. The model also utilizes gates $\alpha_t = \exp(-a \text{ softplus}(\mathbf{W}_\alpha \mathbf{x} +$
238 $b))$ and $\beta_t = \sigma(\mathbf{W}_\beta \mathbf{x})$ to control the state dynamics, where a and b are learnable scalars.
239

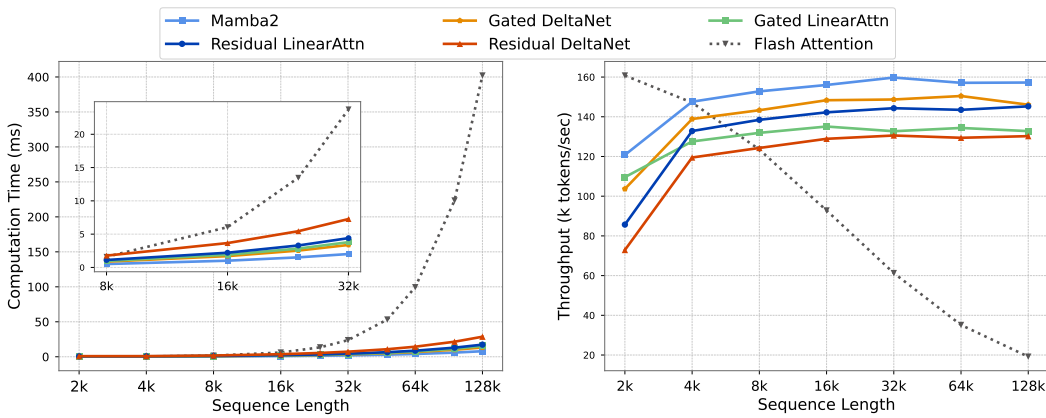
260 4 EXPERIMENT
261262 4.1 SETUP
263

264 **Implementation** To maximize efficiency, we implement our custom attention kernels in Triton
265 (Tillet et al., 2019), building upon the `flash-linear-attention` library (Yang & Zhang,
266 2024). We exploit the fact that our state update rule is identical to linear attention’s, requiring only
267 a minor modification to their kernel: we augment it to return both the attention result and the
268 intermediate residual. This design allows the same highly optimized kernel to be reused across all
269 residual-fitting stages, ensuring high throughput.

270 **Model Settings** We evaluate our model against several recent linear attention architectures, including Retentive Network (RetNet) (Sun et al., 2023), Mamba2 (Dao & Gu, 2024), and Gated Delta Net (GDN) (Yang et al., 2024a). Additionally, we establish a baseline for RLA by evaluating scalar-gated linear attention (sGLA), a linear attention variant equipped with query-key normalization and scalar gates (α and β). In our main experiments, we set the clipping threshold to $c = 1$. All models contain approximately 1.5 billion parameters and are trained on 100 billion tokens under identical conditions to ensure a fair comparison. Further details on the training configuration can be found in Appendix C.

279 4.2 MAIN RESULTS

281 **Kernel Efficiency** We benchmark our kernel’s runtime against linear attention baselines and 282 FlashAttention (Dao et al., 2022; Dao, 2023), as shown in Figure 2. Although the residual fitting 283 process adds computational overhead, our method’s runtime scales linearly with sequence length. This 284 makes it significantly faster than FlashAttention, which scales quadratically, on longer sequences. 285 Regarding throughput, our method, like other linear attention mechanisms, maintains a nearly 286 constant high throughput. Conversely, the throughput of the compute-bound FlashAttention degrades 287 rapidly as sequence length increases.



302 Figure 2: Comparison of attention kernel computation time (left) and model throughput (right) with respect to 303 sequence length.

305 **Language Modeling & Commonsense Reasoning** We evaluate RLA and RDN on Wiki- 306 Text (Merity et al., 2016) perplexity and a suite of benchmarks assessing reasoning and common- 307 sense understanding. The reasoning tasks include ARC-Easy, ARC-Challenge (Clark et al., 2018), 308 PIQA (Bisk et al., 2020), and MMLU (Hendrycks et al., 2020), while commonsense understanding is 309 evaluated on HellaSwag (Zellers et al., 2019), Winogrande (Sakaguchi et al., 2021), SocialIQA (Sap 310 et al., 2019), and LAMBADA (Paperno et al., 2016). Our main results, summarized in Table 2, show 311 that our proposed residual learning variants, RLA and RDN, achieve a consistent improvement in 312 perplexity over their respective baselines, sGLA and GDN. In addition, our models outperform other 313 leading linear attention methods across multiple benchmarks and deliver performance competitive 314 with a standard Transformer.

316 **Recall-intensive tasks** To evaluate memory capacity, we benchmark our model on the recall- 317 intensive tasks from Arora et al. (2024). In addition, we also directly evaluate the model’s retrieval 318 ability using the “Needle-in-a-Haystack” task (NIAH) (gkamradt, 2023), which requires retrieving 319 key-value pairs inserted at varying depths within a long document. These benchmarks are challeng- 320 ing for linear attention models because their finite state-space creates an information bottleneck, as 321 shown in Table 3. Results demonstrate that our proposed RLA and RDN consistently outperform 322 their corresponding baselines, with particularly strong gains on the DROP and FDA benchmarks. 323 Furthermore, they substantially outperform other models on the NIAH task, highlighting an en- 324 hanced capacity for information recall.

324 Table 2: Language modeling, reasoning, and commonsense understanding results. We report perplexity (lower
 325 is better) and accuracy (higher is better). The **bold**/underlined numbers indicate the first/second best values of
 326 the linear attention models in each column.

Model	Wiki ppl	LAMB ppl	ARC-C acc_n	ARC-E acc	HellaSwag acc_n	LAMB acc	MMLU acc_n	PIQA acc	SIQA acc	Wino acc	Avg Acc
Transformer	17.33	19.53	30.2	55.7	49.0	44.3	31.1	70.4	37.9	53.5	46.51
RetNet	18.86	27.62	29.4	56.0	40.5	36.5	30.3	69.9	36.0	50.9	43.69
Mamba2	18.42	20.80	29.1	<u>57.4</u>	46.2	42.7	30.9	69.4	37.6	<u>51.0</u>	45.54
sGLA	17.63	18.06	30.1	56.9	46.4	44.6	30.9	70.4	36.7	50.3	45.79
GDN	<u>17.27</u>	15.76	<u>30.8</u>	54.0	46.8	44.0	<u>31.3</u>	<u>71.3</u>	<u>38.1</u>	51.9	46.03
RLA (ours)	17.35	<u>15.59</u>	30.6	56.6	48.1	<u>46.3</u>	31.0	70.7	38.5	49.7	<u>46.44</u>
RDN (ours)	16.57	14.93	32.1	58.7	47.7	48.7	31.6	71.7	37.7	49.5	47.20

337 Table 3: Accuracy on recall-intensive benchmarks. The **bold**/underlined numbers indicate the first/second best
 338 values of the linear attention models in each column.

Model	DROP	FDA	NQ	SQD	SWDE	TQA	NIAH	Avg
Transformer	26.9	63.0	29.8	35.7	68.7	43.6	70.5	48.31
RetNet	26.2	35.3	20.8	31.5	44.1	39.9	65.7	37.64
Mamba2	26.2	41.2	23.6	<u>33.0</u>	<u>63.4</u>	<u>43.2</u>	67.2	42.54
sGLA	25.7	<u>51.8</u>	24.8	31.6	<u>63.4</u>	41.5	76.6	45.06
GDN	25.9	47.4	26.8	32.4	63.3	43.5	75.7	44.99
RLA (ours)	<u>26.5</u>	51.5	25.2	33.6	64.4	42.3	83.6	<u>46.73</u>
RDN (ours)	27.8	57.5	<u>26.3</u>	32.5	<u>63.4</u>	43.1	<u>79.2</u>	47.11

350 4.3 ABLATION STUDY

352 In this section, we present a series of ablation studies to verify the contributions of key components.
 353 We first quantify the advantage of our learned residual fitting approach over a predefined correction.
 354 Next, we investigate the importance of using a dedicated correction factor, followed by an analysis of
 355 the necessity of the gated mechanism for combining the base prediction and the correction. Finally,
 356 we examine the effect of normalization and residual clipping.

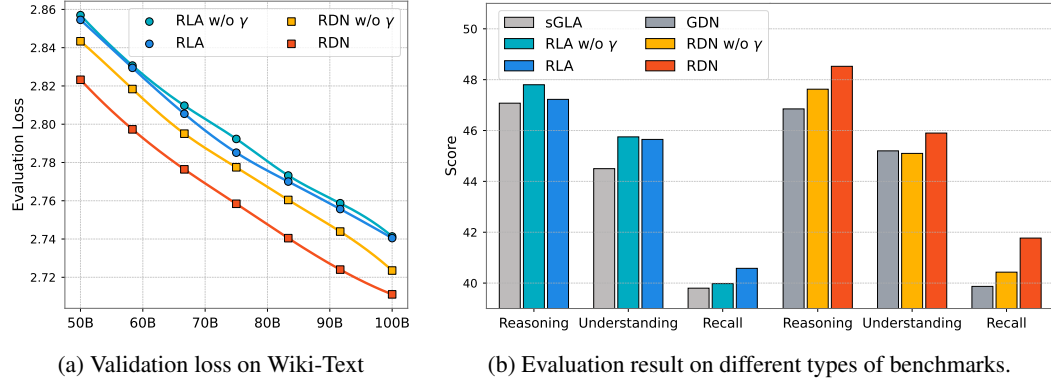
358 **Residual Fitting** To validate the importance of accumulating past errors, we test a variant that
 359 uses a simpler, predefined correction term. In this ablation, we replace our persistent auxiliary state,
 360 \mathbf{R}_t , with a stateless correction derived only from the current residual, $\mathbf{R}_t = (\mathbf{v}_t - \mathbf{S}_{t-1}\mathbf{k}_t)\mathbf{k}_t^\top$.
 361 As demonstrated in Table 4, the variant lacking explicit residual fitting underperforms our full
 362 method. Although this ablated variant maintains competitive performance on some benchmarks,
 363 it exhibits a substantial increase in perplexity on both the training and evaluation sets. This per-
 364 formance drop extends to specialized domains, with a substantial degradation in its math and code
 365 abilities, as measured by perplexity on GSM8k (Cobbe et al., 2021) and HumanEval (Chen et al.,
 366 2021). This demonstrates the critical role of the auxiliary state in accumulating past residuals to
 367 refine the model’s output effectively.

368 Table 4: Ablation study of the residual fitting process, comparing training loss and perplexity across various
 369 datasets. All models were pretrained for 50B tokens with the same hyperparameters, and the best results are
 370 shown in **bold**.

	Training loss	WikiText ppl	LAMB ppl	GSM8k ppl	HumanEval ppl
RLA	2.22	18.76	23.44	3.92	9.61
RLA w/o fitting	2.26	20.19	22.50	6.85	16.23

376 **Dedicated Correction Factor** We analyze the benefit of using a dedicated correction factor, γ ,
 377 by comparing our full models against variants where γ is tied to the update factor β . In Figure 3a,

378 the models with an independent γ consistently achieve lower evaluation loss, with the RDN variant
 379 showing greater improvement. This trend extends to downstream performance, as demonstrated by
 380 the results in Figure 3b, which also show that the dedicated correction factor yields performance
 381 gains across multiple benchmarks. Notably, our foundational architecture, which does not require
 382 an additional γ , still marks a notable improvement over the baseline linear attention method.
 383



395 Figure 3: Ablation study on the correction factor γ . Using a dedicated γ consistently lowers validation loss
 396 compared to tying it to β . The evaluation uses the same benchmarks as in Section 4.2, divided into three task
 397 types, and confirms that a dedicated γ improves performance across several categories.
 398

401 **Gated Output Combination** We conducted an ablation study to analyze the effect of the output
 402 combination formula. This involved comparing our full model, which uses a gated combination of
 403 the base prediction and the error correction ($\mathbf{o}_t = \alpha_t \mathbf{S}_{t-1} \mathbf{q}_t + \gamma_t \mathbf{R}_t \mathbf{q}_t$), against a variant using
 404 simple addition ($\mathbf{o}_t = \mathbf{S}_{t-1} \mathbf{q}_t + \mathbf{R}_t \mathbf{q}_t$). As shown in Table 5, removing the gate causes a slight
 405 performance drop for RDN but a slight increase for RLA. This outcome indicates that the core
 406 benefit is derived from the residual fitting process on the auxiliary state \mathbf{R}_t , rather than the specific
 407 weight used to integrate the correction term.
 408

409 Table 5: Ablation study of different output combination methods. All models share the same 50B tokens
 410 pretraining and hyperparameters, with the best results for each method shown in **bold**.
 411

	Output Combination	ARC-C	ARC-E	HellaSwag	LAMB	MMLU	PIQA	SIQA	Wino	Avg
		acc_n	acc	acc_n	acc	acc_n	acc	acc	acc	
RLA	$\alpha_t \mathbf{S}_{t-1} \mathbf{q}_t + \gamma_t \mathbf{R}_t \mathbf{q}_t$	28.5	53.6	42.0	36.8	29.8	68.6	38.1	49.2	43.30
	$\mathbf{S}_{t-1} \mathbf{q}_t + \mathbf{R}_t \mathbf{q}_t$	28.9	55.2	41.5	37.0	30.1	68.9	37.3	51.6	43.81
RDN	$\alpha_t \mathbf{S}_{t-1} \mathbf{q}_t + \gamma_t \mathbf{R}_t \mathbf{q}_t$	29.8	55.2	42.5	39.9	30.4	69.1	40.4	49.9	44.65
	$\mathbf{S}_{t-1} \mathbf{q}_t + \mathbf{R}_t \mathbf{q}_t$	27.8	56.3	41.9	39.7	29.4	70.0	37.7	48.9	43.96

420 **Normalization and Residual Clipping** Finally, we investigate the importance of normalization
 421 and residual clipping. We perform an ablation study on RLA by removing normalization and
 422 clipping. As shown in Figure 4, both components are crucial for stable training; their removal leads to
 423 unbounded activations and degraded performance. In contrast, the RDN model is largely insensitive
 424 to residual clipping. This robustness is attributable to the inherent stability of its delta rule update,
 425 which maintains a consistent loss curve without residual clipping (Figure 4b).
 426

5 RELATED WORKS

429 Sequence modeling has been historically dominated by Recurrent Neural Networks (RNNs) (Lipton
 430 et al., 2015), including variants like Long Short-Term Memory (LSTM) (Hochreiter & Schmidhuber,
 431 1997) and Gated Recurrent Units (GRU) (Cho et al., 2014). While effective, their inherently
 sequential nature impedes training parallelization. The Transformer architecture (Vaswani et al.,

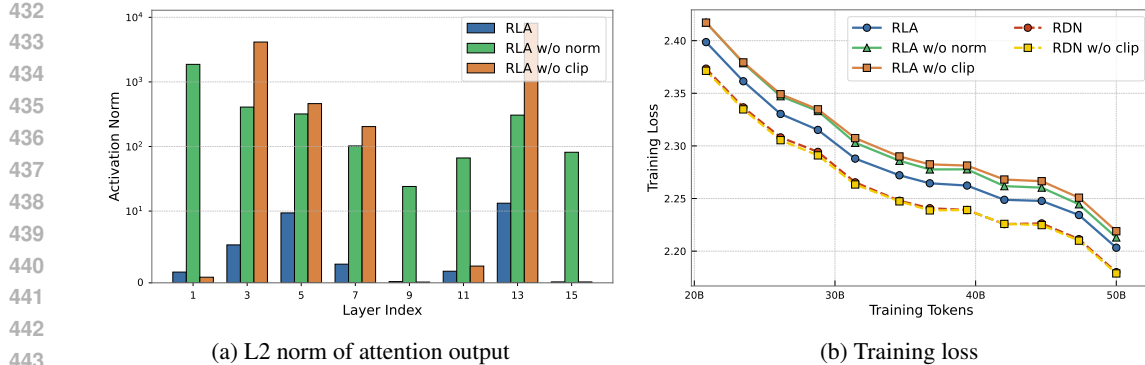


Figure 4: Ablation study on normalization and residual clipping. RLA variants without normalization or clipping exhibit exploding activation norms, indicating training instability. This instability leads to a higher training loss, highlighting that both components are crucial for stable training and better performance. In contrast, residual clipping has a negligible impact on the RDN training process.

2017) overcame this limitation, emerging as the de facto standard for sequence modeling. However, its self-attention mechanism, with a computational complexity quadratic in sequence length, poses a significant bottleneck for long-context applications.

To address these challenges, recent research has revisited Linear RNNs as a foundation for efficient Transformer alternatives. By formulating sequence processing as a linear recurrence, these models achieve both parallelizable training and linear-time inference. Early explorations in this domain, such as S4 (Gu et al., 2021), LRU (Orvieto et al., 2023), and RetNet (Sun et al., 2023), utilized structured state transition matrices. A subsequent performance leap was achieved by incorporating data-dependent dynamics. Models like Mamba (Gu & Dao, 2023; Dao & Gu, 2024), HGRN (Qin et al., 2023; 2024b), and Gated Linear Attention (Yang et al., 2023) leverage input-dependent gating to dynamically control state transitions, thereby enhancing their expressive power.

More advanced methods have introduced the delta learning rule, which reframes the state update from a simple gated decay to a fine-grained memory correction. This approach, exemplified by DeltaNet (Yang et al., 2024b; Schlag et al., 2021) and Gated DeltaNet (Yang et al., 2024a), enables more precise dynamic memory modifications. This mechanism can be interpreted from an online learning perspective, where the state update is framed as an optimization process, as explored in TTT (Sun et al., 2024). This viewpoint has inspired further work aimed at discovering and improving the intrinsic learning algorithms within sequence models (von Oswald et al., 2023; 2025).

Concurrent research has focused on increasing the expressivity of the state transition. For instance, RWKV-7 (Peng et al., 2025) employs a diagonal-plus-low-rank structure, while DeltaProduct (Siems et al., 2025) generalizes DeltaNet by performing multiple update steps per token. To push capacity even further, recent architectures such as Titans (Behrouz et al., 2024) and Miras (Behrouz et al., 2025) have introduced non-linear deep memory, parameterizing the state with an MLP.

6 CONCLUSION

In this paper, we introduced Residual Linear Attention, a framework that enhances linear attention models with an explicit residual fitting process. Our method leverages an auxiliary state to correct the predictive errors of the base model, thereby building more robust and accurate contextual representations. The framework is highly adaptable and can be applied to various linear attention methods. Our experiments demonstrated this versatility, showing that our approach consistently outperforms their respective baselines. While this improvement comes at the cost of additional computation for the fitting process, balancing this trade-off offers a promising direction for future research.

486 REPRODUCIBILITY STATEMENT
487488 To ensure the reproducibility of our research, we will make our resources publicly available. The
489 complete source code is provided in the supplementary material. Our evaluation is conducted using
490 the lm-evaluation-harness (Gao et al., 2024) framework to ensure fair and consistent com-
491 parison with prior work. Details regarding our experimental setup are described in Section 4.1, and
492 a list of model parameters and hyperparameters can be found in Appendix C.
493494 USE OF LARGE LANGUAGE MODELS
495496 We would like to thank Google’s Gemini for its assistance in editing this manuscript. Its suggestions
497 were used to improve grammar, spelling, and overall clarity. The authors reviewed all modifications
498 and take full responsibility for the content of this paper.
499500 REFERENCES
501

502 Simran Arora, Aman Timalsina, Aaryan Singhal, Benjamin Spector, Sabri Eyuboglu, Xinyi Zhao,
503 Ashish Rao, Atri Rudra, and Christopher Ré. Just read twice: closing the recall gap for recurrent
504 language models. *arXiv preprint arXiv:2407.05483*, 2024.

505 Ali Behrouz, Peilin Zhong, and Vahab Mirrokni. Titans: Learning to memorize at test time. *arXiv
506 preprint arXiv:2501.00663*, 2024.

507 Ali Behrouz, Meisam Razaviyayn, Peilin Zhong, and Vahab Mirrokni. It’s all connected: A jour-
508 ney through test-time memorization, attentional bias, retention, and online optimization. *arXiv
509 preprint arXiv:2504.13173*, 2025.

510 Yonatan Bisk, Rowan Zellers, Jianfeng Gao, Yejin Choi, et al. Piqa: Reasoning about physical com-
511 monsense in natural language. In *Proceedings of the AAAI conference on artificial intelligence*,
512 volume 34, pp. 7432–7439, 2020.

513 Mark Chen, Jerry Tworek, Heewoo Jun, Qiming Yuan, Henrique Ponde De Oliveira Pinto, Jared
514 Kaplan, Harri Edwards, Yuri Burda, Nicholas Joseph, Greg Brockman, et al. Evaluating large
515 language models trained on code. *arXiv preprint arXiv:2107.03374*, 2021.

516 Kyunghyun Cho, Bart Van Merriënboer, Caglar Gulcehre, Dzmitry Bahdanau, Fethi Bougares, Hol-
517 ger Schwenk, and Yoshua Bengio. Learning phrase representations using rnn encoder-decoder
518 for statistical machine translation. *arXiv preprint arXiv:1406.1078*, 2014.

519 Peter Clark, Isaac Cowhey, Oren Etzioni, Tushar Khot, Ashish Sabharwal, Carissa Schoenick, and
520 Oyvind Tafjord. Think you have solved question answering? try arc, the ai2 reasoning challenge.
521 *arXiv preprint arXiv:1803.05457*, 2018.

522 Karl Cobbe, Vineet Kosaraju, Mohammad Bavarian, Mark Chen, Heewoo Jun, Lukasz Kaiser,
523 Matthias Plappert, Jerry Tworek, Jacob Hilton, Reiichiro Nakano, et al. Training verifiers to
524 solve math word problems. *arXiv preprint arXiv:2110.14168*, 2021.

525 Tri Dao. Flashattention-2: Faster attention with better parallelism and work partitioning. *arXiv
526 preprint arXiv:2307.08691*, 2023.

527 Tri Dao and Albert Gu. Transformers are ssms: Generalized models and efficient algorithms through
528 structured state space duality. *arXiv preprint arXiv:2405.21060*, 2024.

529 Tri Dao, Dan Fu, Stefano Ermon, Atri Rudra, and Christopher Ré. Flashattention: Fast and memory-
530 efficient exact attention with io-awareness. *Advances in neural information processing systems*,
531 35:16344–16359, 2022.

532 Leo Gao, Jonathan Tow, Baber Abbasi, Stella Biderman, Sid Black, Anthony DiPofi, Charles Fos-
533 ter, Laurence Golding, Jeffrey Hsu, Alain Le Noac’h, Haonan Li, Kyle McDonell, Niklas Muen-
534 nighoff, Chris Ociepa, Jason Phang, Laria Reynolds, Hailey Schoelkopf, Aviya Skowron, Lintang
535 Sutawika, Eric Tang, Anish Thite, Ben Wang, Kevin Wang, and Andy Zou. The language model
536 evaluation harness, 07 2024. URL <https://zenodo.org/records/12608602>.

540 gkamradt. Llmtest needle in a haystack - pressure testing llms. https://github.com/gkamradt/LLMTest_NeedleInAHaystack, 2023.

541

542

543 Albert Gu and Tri Dao. Mamba: Linear-time sequence modeling with selective state spaces. *arXiv preprint arXiv:2312.00752*, 2023.

544

545 Albert Gu, Karan Goel, and Christopher Ré. Efficiently modeling long sequences with structured state spaces. *arXiv preprint arXiv:2111.00396*, 2021.

546

547 Dan Hendrycks, Collin Burns, Steven Basart, Andy Zou, Mantas Mazeika, Dawn Song, and Jacob Steinhardt. Measuring massive multitask language understanding. *arXiv preprint arXiv:2009.03300*, 2020.

548

549

550

551 Sepp Hochreiter and Jürgen Schmidhuber. Long short-term memory. *Neural computation*, 9(8): 552 1735–1780, 1997.

553

554 Angelos Katharopoulos, Apoorv Vyas, Nikolaos Pappas, and François Fleuret. Transformers are 555 rnns: Fast autoregressive transformers with linear attention. In *International conference on machine 556 learning*, pp. 5156–5165. PMLR, 2020.

557

558 Haoyang Li, Yiming Li, Anxin Tian, Tianhao Tang, Zhanhao Xu, Xuejia Chen, Nicole Hu, Wei 559 Dong, Qing Li, and Lei Chen. A survey on large language model acceleration based on kv cache 560 management. *arXiv preprint arXiv:2412.19442*, 2024.

561

562 Zachary C Lipton, John Berkowitz, and Charles Elkan. A critical review of recurrent neural networks 563 for sequence learning. *arXiv preprint arXiv:1506.00019*, 2015.

564

565 Bo Liu, Rui Wang, Lemeng Wu, Yihao Feng, Peter Stone, and Qiang Liu. Longhorn: State space 566 models are amortized online learners. *arXiv preprint arXiv:2407.14207*, 2024.

567

568 Stephen Merity, Caiming Xiong, James Bradbury, and Richard Socher. Pointer sentinel mixture 569 models. *arXiv preprint arXiv:1609.07843*, 2016.

570

571 Antonio Orvieto, Samuel L Smith, Albert Gu, Anushan Fernando, Caglar Gulcehre, Razvan Pas- 572 canu, and Soham De. Resurrecting recurrent neural networks for long sequences. In *International 573 Conference on Machine Learning*, pp. 26670–26698. PMLR, 2023.

574

575 Denis Paperno, Germán Kruszewski, Angeliki Lazaridou, Quan Ngoc Pham, Raffaella Bernardi, 576 Sandro Pezzelle, Marco Baroni, Gemma Boleda, and Raquel Fernández. The lambada dataset: 577 Word prediction requiring a broad discourse context. *arXiv preprint arXiv:1606.06031*, 2016.

578

579 Bo Peng, Ruichong Zhang, Daniel Goldstein, Eric Alcaide, Xingjian Du, Haowen Hou, Jiaju Lin, 580 Jiaxing Liu, Janna Lu, William Merrill, et al. Rwkv-7" goose" with expressive dynamic state 581 evolution. *arXiv preprint arXiv:2503.14456*, 2025.

582

583 Zhen Qin, Songlin Yang, and Yiran Zhong. Hierarchically gated recurrent neural network for 584 sequence modeling. *Advances in Neural Information Processing Systems*, 36:33202–33221, 2023.

585

586 Zhen Qin, Weigao Sun, Dong Li, Xuyang Shen, Weixuan Sun, and Yiran Zhong. Various 587 lengths, constant speed: Efficient language modeling with lightning attention. *arXiv preprint 588 arXiv:2405.17381*, 2024a.

589

590 Zhen Qin, Songlin Yang, Weixuan Sun, Xuyang Shen, Dong Li, Weigao Sun, and Yiran Zhong. 591 Hgrn2: Gated linear rnns with state expansion. *arXiv preprint arXiv:2404.07904*, 2024b.

592

593 Keisuke Sakaguchi, Ronan Le Bras, Chandra Bhagavatula, and Yejin Choi. Winogrande: An adver- 594 sarial winograd schema challenge at scale. *Communications of the ACM*, 64(9):99–106, 2021.

595

596 Maarten Sap, Hannah Rashkin, Derek Chen, Ronan LeBras, and Yejin Choi. Socialqa: Common- 597 sense reasoning about social interactions. *arXiv preprint arXiv:1904.09728*, 2019.

598

599 Imanol Schlag, Kazuki Irie, and Jürgen Schmidhuber. Linear transformers are secretly fast weight 600 programmers. In *International conference on machine learning*, pp. 9355–9366. PMLR, 2021.

594 Julien Siems, Timur Carstensen, Arber Zela, Frank Hutter, Massimiliano Pontil, and Riccardo
 595 Grazzi. Deltaproduct: Improving state-tracking in linear rnns via householder products. *arXiv*
 596 *preprint arXiv:2502.10297*, 2025.

597

598 Yu Sun, Xinhao Li, Karan Dalal, Jiarui Xu, Arjun Vikram, Genghan Zhang, Yann Dubois, Xinlei
 599 Chen, Xiaolong Wang, Sanmi Koyejo, et al. Learning to (learn at test time): Rnns with expressive
 600 hidden states. *arXiv preprint arXiv:2407.04620*, 2024.

601

602 Yutao Sun, Li Dong, Shaohan Huang, Shuming Ma, Yuqing Xia, Jilong Xue, Jianyong Wang, and
 603 Furu Wei. Retentive network: A successor to transformer for large language models. *arXiv*
 604 *preprint arXiv:2307.08621*, 2023.

605

606 Philippe Tillet, Hsiang-Tsung Kung, and David Cox. Triton: an intermediate language and compiler
 607 for tiled neural network computations. In *Proceedings of the 3rd ACM SIGPLAN International
 608 Workshop on Machine Learning and Programming Languages*, pp. 10–19, 2019.

609

610 Ashish Vaswani, Noam Shazeer, Niki Parmar, Jakob Uszkoreit, Llion Jones, Aidan N Gomez,
 611 Łukasz Kaiser, and Illia Polosukhin. Attention is all you need. *Advances in neural informa-*
 612 *613 tion processing systems*, 30, 2017.

614

615 Johannes von Oswald, Maximilian Schlegel, Alexander Meulemans, Seijin Kobayashi, Eyyvind
 616 Niklasson, Nicolas Zucchet, Nino Scherrer, Nolan Miller, Mark Sandler, Max Vladymyrov, et al.
 617 Uncovering mesa-optimization algorithms in transformers. *arXiv preprint arXiv:2309.05858*,
 618 2023.

619

620 Johannes von Oswald, Nino Scherrer, Seijin Kobayashi, Luca Versari, Songlin Yang, Maxi-
 621 milian Schlegel, Kaitlin Maile, Yanick Schimpf, Oliver Sieberling, Alexander Meulemans,
 622 et al. Mesanet: Sequence modeling by locally optimal test-time training. *arXiv preprint*
 623 *arXiv:2506.05233*, 2025.

624

625 Songlin Yang and Yu Zhang. Fla: A triton-based library for hardware-efficient implementations
 626 of linear attention mechanism, January 2024. URL [https://github.com/fla-org/](https://github.com/fla-org/flash-linear-attention)
 627 [flash-linear-attention](https://github.com/fla-org/flash-linear-attention).

628

629 Songlin Yang, Bailin Wang, Yikang Shen, Rameswar Panda, and Yoon Kim. Gated linear attention
 630 transformers with hardware-efficient training. *arXiv preprint arXiv:2312.06635*, 2023.

631

632 Songlin Yang, Jan Kautz, and Ali Hatamizadeh. Gated delta networks: Improving mamba2 with
 633 delta rule. *arXiv preprint arXiv:2412.06464*, 2024a.

634

635

636 Songlin Yang, Bailin Wang, Yu Zhang, Yikang Shen, and Yoon Kim. Parallelizing linear transform-
 637 ers with the delta rule over sequence length. *Advances in neural information processing systems*,
 638 37:115491–115522, 2024b.

639

640 Rowan Zellers, Ari Holtzman, Yonatan Bisk, Ali Farhadi, and Yejin Choi. Hellaswag: Can a ma-
 641 chine really finish your sentence? *arXiv preprint arXiv:1905.07830*, 2019.

642

643

644

645

646

647

648 A UNIFIED FORMULA FOR RESIDUAL LINEAR ATTENTION
649650 This section details how our residual fitting process can be framed as a form of online gradient
651 boosting, providing a unified and extensible framework.
652653 A.1 PRELIMINARY: GRADIENT BOOSTING IN A FUNCTIONAL SPACE
654655 Gradient boosting is an ensemble technique that sequentially adds new models to correct the errors
656 of previous ones. In a gradient boosting framework, the objective at each stage is to find a new
657 function h that minimizes the loss when added to the current function f :
658

659
$$h^* = \arg \min_h \mathbb{E}_{\mathbf{k}, \mathbf{v}} [\mathcal{L}(f(\mathbf{k}) + h(\mathbf{k}), \mathbf{v})].$$

660

661 As finding the optimal function h is generally infeasible, we approximate the objective using a first-
662 order Taylor expansion of the loss:
663

664
$$\mathcal{L}(f(\mathbf{k}) + h(\mathbf{k}), \mathbf{v}) \approx \mathcal{L}(f(\mathbf{k}), \mathbf{v}) + h(\mathbf{k}) \frac{\partial \mathcal{L}(f(\mathbf{k}), \mathbf{v})}{\partial f(\mathbf{k})}.$$

665

666 The direction of steepest descent in this functional space is the negative gradient of the loss with
667 respect to the function's output. This target is often called a pseudo-residual, \mathbf{r} :
668

669
$$\mathbf{r} = -\frac{\partial \mathcal{L}(f(\mathbf{k}) + h(\mathbf{k}), \mathbf{v})}{\partial h(\mathbf{k})} \approx -\frac{\partial \mathcal{L}(f(\mathbf{k}), \mathbf{v})}{\partial f(\mathbf{k})}.$$

670
671

672 The objective thus becomes learning a function $h(\mathbf{k})$ that fits this pseudo-residual. After learning,
673 the boosted function is updated as $f(\mathbf{k}) \leftarrow f(\mathbf{k}) + h(\mathbf{k})$, where $h(\mathbf{k})$ is the error correction term.
674675 A.2 UNIFIED RESIDUAL LINEAR ATTENTION
676677 From an online learning perspective, linear attention can be viewed as learning a mapping $f(\mathbf{k}; \mathbf{S})$,
678 where the state matrix \mathbf{S} is incrementally updated via online gradient descent to minimize a loss
679 $\mathcal{L}(f(\mathbf{k}; \mathbf{S}), \mathbf{v})$. We enhance this model by incorporating principles from gradient boosting. This
680 involves employing an auxiliary state matrix \mathbf{R} for iterative refinement. In this framework, state
681 matrix \mathbf{R} is updated at timestep t to learn the mapping from the key \mathbf{k}_t to the pseudo-residual \mathbf{r}_t of
682 the prior prediction. This correction process results in a stronger mapping function.683 We can decouple the learning objective into two parts: (1) A global objective, defined by an arbi-
684 trary, differentiable outer loss $\mathcal{L}_{\text{outer}}$, which sets the overall key-to-value mapping goal. (2) A local
685 objective, defined by a simple inner loss $\mathcal{L}_{\text{inner}}$, which governs how each individual state matrix is
686 updated. While the target pseudo-residual \mathbf{r} can be complex, the task for each state is deliberately
687 kept simple. Ignoring decay factors and learning rates for clarity, the general recurrence is:
688

689
$$\mathbf{r}_t = -\frac{\partial \mathcal{L}_{\text{outer}}(f(\mathbf{k}_t; \mathbf{S}_{t-1}), \mathbf{v}_t)}{\partial f(\mathbf{k}_t; \mathbf{S}_{t-1})} \quad (\text{Pseudo-Residual})$$

690
691

692
$$\mathbf{R}_t = \mathbf{R}_{t-1} - \frac{\partial \mathcal{L}_{\text{inner}}(f(\mathbf{k}_t; \mathbf{R}_{t-1}), \mathbf{r}_t)}{\partial \mathbf{R}_{t-1}} \quad (\text{Auxiliary State Update})$$

693
694

695
$$\mathbf{S}_t = \mathbf{S}_{t-1} - \frac{\partial \mathcal{L}_{\text{inner}}(f(\mathbf{k}_t; \mathbf{S}_{t-1}), \mathbf{v}_t)}{\partial \mathbf{S}_{t-1}} \quad (\text{Base State Update})$$

696
697

698
$$\mathbf{o}_t = f(\mathbf{q}_t; \mathbf{S}_{t-1}) + f(\mathbf{q}_t; \mathbf{R}_t) \quad (\text{Base Prediction and Correction})$$

699

700 The gating mechanism and correction strength can also be easily incorporated into the framework.
701 This framework allows two simple inner update rules to approximate a more complex global objec-
702 tive.

702 **B RESIDUAL FITTING WITH HUBER LOSS**
 703

704 As previously established, our framework can accommodate complex global loss functions, as their
 705 complexity is confined to the pseudo-residual calculation. This allows us to use a more robust
 706 alternative to the standard L2 loss, such as the Huber loss function:
 707

708
$$\mathcal{L}_{\text{huber}}(\hat{\mathbf{v}}, \mathbf{v}) = \sum_{i=1}^d \mathcal{L}_{\text{huber}}(\hat{v}_i, v_i),$$

 709
 710
 711

712 where $\mathcal{L}_{\text{huber}}(\hat{v}_i, v_i) = \begin{cases} \frac{1}{2}(v_i - \hat{v}_i)^2 & \text{for } |v_i - \hat{v}_i| \leq c \\ c(|v_i - \hat{v}_i| - \frac{1}{2}c) & \text{for } |v_i - \hat{v}_i| > c \end{cases}$
 713
 714

715 This function uses the L2 loss for small errors and the L1 loss for large errors, making it a more
 716 robust alternative. Directly applying this loss yields a non-linear update rule that is difficult to
 717 parallelize:
 718

719
$$\mathbf{S}_t = \mathbf{S}_{t-1} - \frac{\partial \mathcal{L}_{\text{huber}}(\mathbf{v}_t - \mathbf{S}_{t-1} \mathbf{k}_t)}{\partial \mathbf{S}_{t-1}}$$

 720
 721
 722
$$= \mathbf{S}_{t-1} + \text{Clip}_{[-c, c]}(\mathbf{v}_t - \mathbf{S}_{t-1} \mathbf{k}_t) \mathbf{k}_t^\top$$

 723

724 Our residual fitting framework elegantly avoids this problem. The complexity is isolated within the
 725 pseudo-residual calculation, while the core state update remains simple. The pseudo-residual for the
 726 Huber Loss is $\mathbf{r}_t = \text{Clip}_{[-c, c]}(\mathbf{v}_t - f(\mathbf{k}_t; \mathbf{S}_{t-1}))$, then the inner update rule is only responsible for
 727 fitting this target pseudo-residual. Using an inner loss of $\mathcal{L}_{\text{inner}}(f(\mathbf{k}), \mathbf{v}) = -\langle \mathbf{v}, f(\mathbf{k}) \rangle$ yields the
 728 following recurrence:
 729

730
$$\mathbf{r}_t = \text{Clip}_{[-1, 1]}(\mathbf{v}_t - \mathbf{S}_{t-1} \mathbf{k}_t)$$

 731
 732
 733
$$\mathbf{R}_t = \mathbf{R}_{t-1} - \mathbf{r}_t \mathbf{k}_t^\top$$

 734
 735
$$\mathbf{S}_t = \mathbf{S}_{t-1} - \mathbf{v}_t \mathbf{k}_t^\top$$

 736

737 This equivalence provides the theoretical motivation for our clipping mechanism; it is an efficient
 738 implementation of a robust Huber loss objective, which leads to a more stable residual fitting process.
 739 This principle can be generalized by selecting other robust loss functions. For instance, the Log-
 740 Cosh loss has a negative gradient with respect to the prediction $f(\mathbf{k})$ that is equivalent to applying a
 741 tanh function to the residual:
 742

743
$$\mathcal{L}_{\text{log-cosh}}(f(\mathbf{k}), \mathbf{v}) = \log \cosh(\mathbf{v} - f(\mathbf{k})),$$

 744

$$\mathbf{r}_t = \tanh(\mathbf{v}_t - f(\mathbf{k}_t; \mathbf{S}_{t-1})).$$

745 This can be viewed as a smooth alternative to the clipped residual from the Huber loss. The ability
 746 to easily substitute such loss functions demonstrates our framework’s modularity, allowing for the
 747 integration of powerful learning objectives while maintaining computational efficiency.
 748

749 **C MODEL STRUCTURE AND TRAINING HYPER PARAMETERS**
 750

751 We evaluate several model architectures, with full specifications detailed in Table 6. Our comparison
 752 includes a standard Transformer and Transformers with pure linear attention. For a fair comparison,
 753 all models are trained using an identical set of hyperparameters, which are listed in Table 7. We
 754 initialize the model weights from a normal distribution with a constant standard deviation and use
 755 the AdamW optimizer with a cosine learning rate schedule for training.

756

Table 6: Model Configuration

757

758

Property	Transformer Models	Linear Attention Models
Total Params	1.51B	1.55B
Hidden Size	2048	2048
Intermediate Size	8192	8192
Attention Heads	32	16
GQA Groups	4	16
Head Dimension	128	128
Softmax Attention Layers	16	0
Linear Attention Layers	0	16

759

760

761

762

763

764

765

766

767

Table 7: Training hyperparameters

768

Peak LR	Min LR	Batch Size	Warmup Tokens	Total Tokens	Weight Decay	Gradient Clip	Initialization Std
3e-4	3e-5	4M	0.5B	100B	0.1	1.0	0.006

769

770

771

D PSEUDO-CODE IMPLEMENTATION

772

773

This section provides a PyTorch-like pseudo-code implementation for our proposed Residual Linear Attention (RLA). We present the recurrent formulation to clearly illustrate our modifications to a baseline scalar-gated linear attention mechanism.

```

1  # q, k, v are in shape [sequence_length, head_dimension].
2  # alpha, beta and gamma are in shape [sequence_length]
3
4  def scalar_gated_linear_attention(q, k, v, alpha, beta):
5      # Recurrently compute linear attention with scalar gates.
6      seq_len, head_dim = q.shape
7      S = torch.zeros(head_dim, head_dim)
8      o = torch.zeros(seq_len, head_dim)
9      for t in range(seq_len):
10          qt, kt, vt = q[t : t + 1], k[t : t + 1], v[t : t + 1]
11          # update state S
12          S = alpha[t] * S + beta[t] * kt.T @ vt
13          # get prediction
14          o[t : t + 1] = qt @ S
15      return o
16
17
18 def residual_linear_attention(q, k, v, alpha, beta, gamma):
19     # Recurrently compute residual linear attention.
20     seq_len, head_dim = q.shape
21     S = torch.zeros(head_dim, head_dim)
22     R = torch.zeros(head_dim, head_dim)
23     o = torch.zeros(seq_len, head_dim)
24     for t in range(seq_len):
25         qt, kt, vt = q[t : t + 1], k[t : t + 1], v[t : t + 1]
26         # l2 normalization
27         qt, kt = F.normalize(qt, dim=-1), F.normalize(kt, dim=-1)
28         # clipped residual error
29         rt = torch.clip(vt - kt @ S, min=-1, max=1)
30         # update auxiliary state R
31         R = alpha[t] * R + gamma[t] * kt.T @ rt
32         # combine basic prediction and error correction
33         o[t : t + 1] = alpha[t] * qt @ S + gamma[t] * qt @ R
34         # update basic state S
35         S = alpha[t] * S + beta[t] * kt.T @ vt
36     return o

```

Listing 1: Pseudo-code for Residual Linear Attention (RLA) and a baseline linear attention model.

808

809